Effects of graphene oxide on the diatom Nitzschia palea are associated with carbon cycling disturbance

Paul Braylé, Eric Pinelli, Benoît Schoefs, Emmanuel Flahaut, Jérôme Silvestre, Laury Gauthier, Maialen Barret

Carbon 226 (2024) 119224

Contents lists available at ScienceDirect

Carbon

journal homepage: www.elsevier.com/locate/carbon

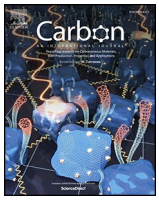

Effects of graphene oxide on the diatom *Nitzschia palea* are associated with carbon cycling disturbance

Paul Braylé [a,*], Eric Pinelli [a], Benoît Schoefs [b], Emmanuel Flahaut [c], Jérôme Silvestre [a], Laury Gauthier [a], Maialen Barret [a]

[a] Centre de Recherche sur La Biodiversité et L'Environnement (CRBE), Université de Toulouse, CNRS, IRD, Toulouse INP, Université Toulouse 3 – Paul Sabatier (UT3), Toulouse, France
[b] Metabolism Microalgal Engineering and Applications (MIMMA), Biologie des Organismes Stress Santé Environnement, IUML – FR 3473 CNRS, Le Mans Université, Le Mans, France
[c] Centre Inter-universitaire de Recherche et D'Ingénierie des Matériaux, Université Toulouse 3 Paul Sabatier, CNRS, Toulouse INP, Toulouse, France

ARTICLE INFO

Keywords:
2D nanoparticle
Microalgae
Biofilm
Photosynthesis
Heterotrophy

ABSTRACT

Graphene based nanomaterials (GBMs) have been drawing the attention of the scientific communities these past years. As their market is increasing every year, their potential environmental and health risk are to be assessed. As microbial communities represent the basis of every ecosystem, it is essential to evaluate the risks of GBMs on these communities. The effects of GBMs on bacteria has been widely studied, while the effects on phototrophic species are less represented. In this study, the diatom *Nitzschia palea* was exposed to graphene oxide (GO) and reduced graphene oxide (rGO), at 0.1, 1 and 10 mg L^{-1}. rGO had no effect on the diatom while GO induced an increase in growth, indicating the importance of the oxidation rate in the observed effect. Further results showed that shading effect of GO was countered by increased chlorophyll contents and by the accumulation of GO into the biofilm. This "sticking" mechanism increased the proximity between the biofilm and the GO, which might favour interactions between GO and the biofilm. These interactions led to the increase of defects and the reduction of GO. In addition, increased heterotrophic activity was suggested. To our knowledge, no diatom before *Nitzschia palea* has been shown to enhance its growth in presence of a GBM, but also capable to modify it. These results demonstrate the potential of GBMs, and in particular those with higher oxidation rates, to disrupt the contribution of the diatom *Nitzschia palea* to carbon cycling, which could have broader consequences at ecosystem scale.

1. Introduction

In 2004, graphene was exfoliated from graphite for the first time by Novoselov and his co-workers [1]. This discovery has led to the emergence of a multitude of graphene-based nanomaterials (GBMs) such as graphene oxide (GO) and reduced graphene oxide (rGO). Thanks to their unique properties, GBMs are used in a wide range of industries for electronics, photonics, clean energy and sensors [2], in regenerative medicine and biomedical devices [3], but also in environmental pollution treatment [4,5]. The applications and the market of graphene and its derivatives are continually growing and their value estimation is ranging from 0.34 to 1.5 billion US dollars in 2027 [6].

Even though GBMs are not yet detectable in the environment, their increased use will lead to their release in the environment such as surface waters. GBMs could be comparable to carbon nanotubes (CNTs), and modelling studies estimate that concentrations of CNTs are estimated between 0.001 and 1000 μg L^{-1} in aquatic systems [7,8]. Microbial communities, especially biofilms, are at the basis of these ecosystems and endorse vital roles such as element cycling. Effect of GBMs on microbial mono species is a trending topic these past years. Showing the effects of GBMs at a community level is more environmentally relevant, but studying effects at single species level is also important in order (i) to understand the mechanisms of action of the nanoparticles and (ii) to determine the tolerance range of the species studied. Biofilms are composed of many species of bacteria, but also micro-algae and diatoms. Effects of GBMs on bacteria are today well documented in the literature and greatly reviewed [3,9,10]. GBMs are described for their antibacterial activity related to oxidative stress, lipid

* Corresponding author.
E-mail address: paul.brayle@gmail.com (P. Braylé).

https://doi.org/10.1016/j.carbon.2024.119224
Received 6 October 2023; Received in revised form 2 May 2024; Accepted 8 May 2024
Available online 12 May 2024

peroxidation but also interactions with DNA. Even though the main effects of GBMs on bacteria are negative, some species seem to be more resistant than others, showing that GBM effects are species dependant. Despite their vital roles in carbon cycling and oxygen production [11], only few studies have been dedicated towards micro algae and especially diatoms. A review of the available literature establishes the negative impact of GBMs on the growth of micro algae, often related to a shading effect affecting the photosynthesis efficiency but also oxidative stress and physical damage [12–17]. Interestingly, in a complex community composed of bacteria and the diatom *Nitzschia palea*, GO had a positive impact on the division rate of the diatoms [18]. These results appeared contradictory with the negative effects on micro algae in multiple studies reported previously. The authors hypothesized a differential balance between autotrophic and heterotrophic metabolism upon GO exposure, or an indirect effect resulting from the interaction with bacteria. Moreover, unlike micro algae studied in the literature, *Nitzschia palea* is benthic and lives in a biofilm embedded in exopolymeric substances (EPS). The study by Evariste et al. paved the way to further investigations on *Nitzschia palea* alone in order to understand the mechanisms of action of GBMs on this diatom and to enrich the literature on the effects of GBMs on benthic microalgae.

In the present study, the effects of GO and rGO at 0.1, 1 and 10 mg L^{-1} were investigated on the diatom *Nitzschia palea*. First of all, the impact of GBMs on the replication capacity was analysed. Then, a series of experiments were done in order to gain insight into the effects of GO on the photosynthetic activities, such as chlorophyll content, shading effect and photosynthesis efficiency. To investigate more deeply the different interactions ongoing between the diatom cells and GO, the "sticking" of GO in the diatom biofilm was quantified and observed. The potential effect of GO on the bioavailability of the medium elements was also investigated. In order to evaluate the possible effects of *N. palea* on GO, RAMAN spectrometry was used for the nanoparticle characterisation. Finally, the possible enhancement of the heterotrophy of the diatom and related lipid contents were analysed.

2. Materials and methods

2.1. Pre-culture of the diatom Nitzschia palea

The diatom used for this experiment is a benthic axenic strain of *Nitzschia palea* CPCC160 provided by the Canadian Physiological Culture Centre of Waterloo University in Canada. The diatom was cultivated in sterile cell culture 100 mL flasks with SPE medium (Falcon 355 001) [13]. Flasks were permanently agitated at 40 rpm at 20 ± 2 °C and exposed under a LED white light delivering 50 μmol photons. m^{-2}. s^{-1} with a cycle of 14 h of light and 10 h of darkness. Culture medium was changed every five days and the absence of bacterial contamination was checked using cytometry analysis with a SYTO9 marker (see 1.4 Cytometry analysis).

2.2. Graphene based materials

Two types of GBMs were used during this experiment: GO and rGO. The GO came from the "Antolin Group", prepared by exfoliation of carbon nanofibers of the "Grupo Antolin Carbon Nanofiber" (GANF®) (Grupo Antolin, Burgos, Spain) followed by an oxidation according to the Hummers' method [19] and used as provided. The rGO was obtained from this same GO by a thermal reduction at 200 °C in a H_2 atmosphere (5 L h^{-1} flow rate), resulting in a partial reduction of the GO. These reduction steps and the characterisation of the different GBMs were all carried out by the "Centre Inter-Universitaire de Recherche et Ingénierie des Materiaux" (CIRIMAT) in Toulouse.

2.3. -medium interaction

In order to evaluate the potential adsorption of chemical elements by GO in the culture medium, 10 mg L^{-1} of GO were incubated in 15 mL of SPE medium for 24 h and 5 replicates were done along with 5 replicates of SPE medium as a control. Samples were then filtered at 0.45 μm and acidified at 5 % HNO_3. Dissolved elements were quantified by ICP-OES (quantification limit: 2–10000 μg kg^{-1}, precision measure: 1–5%; AMETEK Spectro ARCOS FHX22, Kleve, Germany).

2.4. Effect of GO and rGO on diatom division rate, lipid and chlorophyll content

Three concentrations of GO and rGO were tested: 0.1, 1 and 10 mg L^{-1}. Those concentrations were chosen for their environmental relevancy [7,8] and can be comparable with concentrations used in other ecotoxicological tests on micro algae ranging from 0.01 to 300 mg L^{-1} [12–16,20–22]. Exposure to GBMs was carried out in Falcon 6-well culture plates. For each sampling point (0 h, 24 h, 48 h, 96 h, 144 h), three wells (triplicates) of each condition and control were prepared. Two days before exposure, wells were inoculated with 250 000 cells of *N. palea* in 1.5 mL of SPE medium to allow the diatoms to attach to the culture plates. At t0, diatoms were exposed to the different concentrations of GO and rGO and wells were all adjusted to 3 mL with SPE medium. Just before GBM addition, each suspension of GBM was bath sonicated for 1 min in order to redisperse the materials.

In order to evaluate the effect of GO on the heterotrophy of the diatom (part 2.8), the protocol was slightly changed. Plates with control and 10 mg L^{-1} of GO were placed in the dark for 48 h just after the exposure started. Otherwise, all other factors were the same as described above.

At each sampling point, wells were gently scrapped in order to resuspend cells from the biofilm and samples collected from experiments were analysed by flow cytometry using a CytoFLEX© cytometer (Beckman Coulter) with a 488 nm excitation laser. Each experimental condition was analysed in technical triplicates of 200 μL of resuspended culture transferred into 96-well plates. Flow cytometry analysis was carried out on a homogeneous population based on the chlorophyll fluorescence in which reading doublets were avoided. Division rates were calculated using the following equation [23]:

$$\textit{Divison rate} = \frac{\text{Cell concentration at sampling point} - \text{Cell concentration at t0}}{\text{Cell concentration at t0}}$$

Cytometry analysis coupled to fluorescent markers was used to investigate physiological changes in diatoms. Samples were incubated with Bodipy™ 493/503 at 1 μg L^{-1} for 1 min [24] to mark neutral lipids and fluorescence was read at 525 nm. Chlorophyll content was also assessed, based on its natural fluorescence at 610 nm. At each sampling point, bacterial contamination was also investigated using a SYTO9 marker with 15 min of incubation at 5 μM [25].

2.5. Shading effect of GO

The shading effect of GO was measured as described in the literature

[13,23]. The experiment consisted in exposing *Nitzschia palea* to shade induced by GO and by avoiding any contact between the biofilm and the GBM. Two 6-well culture plates were therefore overlayed and placed in a dark box allowing light to pass only through the top side. The bottom plate was inoculated with *Nitzschia palea* while the upper plate contained GO at 10 or 50 mg L^{-1}. Exposure was then conducted as described in 1.4. Division rates and chlorophyll contents were then measured using the flow cytometry protocol detailed in 1.4.

2.6. Photosynthesis efficiency

For the photosynthesis parameters analysis, diatoms were grown in 6-well plates containing either 0 or 10 mg L^{-1} of GO. The exposure conditions were the same as detailed before. In addition to the 0 h, 24 h, 48 h, 96 h and 144 h sampling points, additional sampling points were added each day: 8 h, 32 h, 56 h, 104 h and 152 h. This was done in order to obtain information of the photosynthesis efficiency at the beginning and at the end of the light period. For each sampling point, growth medium was carefully discarded, removing at the same time cells that were not part of the benthic biofilm. Fresh SPE medium was then added (2 mL), and the biofilm was gently resuspended. The resulting suspension was transferred into 2 mL sterile tubes and placed in darkness for 15 min before fast fluorescence measurement using a Dual PAM 100 (Walz, Germany). Different parameters were determined: the maximum fluorescence yield (F_M), the minimal fluorescence yield (F_0) (mean of the fluorescence signal over 200 m s preceding the actinic illumination), the fluorescence yield at 300 μs ($F_{300\mu s}$) (used to determine the initial slope M0 of the relative variable fluorescence kinetics), the fluorescence yield at 2 m s (F_J) and finally the fluorescence yield at 30 m s (F_I). These yields were used to calculate different energy fluxes per reaction centre (RC) (absorption, trapping, dissipation and electron transport) using the equations established by Stirbeta et al. [26].

2.7. 77 k fluorescence spectroscopy

Three replicates of diatoms incubated during 144 h with or without GO (10 mg L^{-1}) were snap frozen in liquid nitrogen for 77 K fluorescence spectrum recording using a PerkinElmer LS-55 B. The original spectra were treated according to the method described by Schoefs et al. [27]. Excitation (440 nm) and emission (600–800 nm) slits were both set at 5 nm.

2.8. Sedimentation and "sticking" of GO

The sedimentation of GBMs was also assessed in 6-well culture plates and the experimental procedure was the same as described in section 1.4. A control without diatoms was also added in order to investigate the kinetics of GO sedimentation without diatom cells. At sampling times (0 h, 6 h, 2 4 h, 48 h, 96 h, 144 h), 1.5 mL of top fraction of the water column was collected and the optical density was determined at 800 nm using a UVisco V-1600 spectrophotometer.

Once the liquid fractions collected, the wells were rinsed with SPE medium in order to remove all GO and diatoms that were not strongly attached in the biofilm. Six images of each well were recorded (18 per condition) using an Olympus SZX10 magnifier coupled with an Olympus SC30 colour camera. The images were then processed in ImageJ (v 1.53 k, Wayne Rasband and contributors, National Institutes of Health, USA) for scaling, converting to a black and white binary images, optimising the colour threshold in order to detect the GO and finally calculating the surface covered by GO.

2.9. Scanning electron microscope (SEM)

To visualize the biofilm, SEM analyses were performed at the "Centre de Microscopie Electronique Appliquée à la Biologie" (CMEAB, Toulouse, France). In order to prepare the *Nitzchia palea* biofilms for SEM analysis, circular glass slides were deposited in the 6 wells of the culture plates. Exposure to GO was the same as described in 1.4. After 144 h of exposure, the medium was removed and wells were rinsed with fresh SPE medium and emptied again. Adherent cells on the glass slides were fixed with 2 % glutaraldehyde in Sörensen buffer at 0.1 M, pH 7.4, for 4 h minimum. The slides were then washed in 3 consecutive water baths of 10 min. They were dehydrated in ascending alcohol solutions (30°, 50°, 70°, 95° for 10 min, and finally 15 min in 100° 3 times). Drying was then done by diverting the CO_2 critical point using a Leica EM CPD 300. Finally, samples were coated with 4–10 nm (60 mA) of platinum with a Leica EM MED020. Once samples were ready, SEM was performed with a FEG Quanta 250 FEI.

2.10. Raman analysis of GO

RAMAN spectrometry was used in order to evaluate possible alterations of GO after exposure with *Nitzschia palea*. Experiments were conducted on GO from experiments after 144 h of exposure in 50 mL SPE in 100 mL Falcon 35 501 flasks at 10 mg L^{-1} of GO. Different "types" of GO were identified for the analysis: the initial GO at 10 mg L^{-1} in SPE medium before exposure (GO 0 h), the GO stuck in the biofilm after 144 h of exposure (GO + diatoms 144 h) and GO that was inoculated in SPE culture medium in absence of diatom cells (GO in SPE 144 h) in order to observe the possible alteration of GO in the medium alone. In order to separate GO from the diatoms, samples were sonicated in water baths for 10 min and deposited and spread on glass slides. All other samples underwent the same sonication and deposition on glass slides. In order to evaluate the possible changes in the RAMAN spectra resulting from interactions with extracellular components and components obtained after sonication, another control was added: diatom lysates were added to the GO 144 h sample just before RAMAN analysis (GO in SPE 144 h + lysate). RAMAN analyses were conducted by the team Equipex-Critex of the "Laboratoire de Chimie Agro-Industrielle" (LCA, INP, Toulouse, France). A LabRAM HR Evolution was used with the following parameters: 532 nm laser, 50 mW, 5 % power reduction filter, ×50 LWD (Olympus) long distance lens, 200 μm confocal hole, 5s acquisition and 7 accumulations. All spectra were then analysed in LabSpec 5 software. The baseline of each spectrum was redefined and the intensity of the D (I_D) and G (I_G) bands (respectively 1350 and 1580 cm^{-1} RAMAN shift) were recorded in order to calculate the I_D/I_G ratio of each GO type. The position of the peak of the different bands did not present any shifts between samples and/or conditions.

2.11. Statistical analysis

All statistical analyses were performed using Rstudio (RStudio 2023.09.1). To determine significant differences between exposure conditions, normality of values and homoscedasticity of variances were tested with a Shapiro and Bartlett test respectively. When comparing three and more groups of values, an ANOVA was performed. When significant differences were underlined by the ANOVA ($p < 0.05$), a TukeyHSD post-hoc test was done in order to highlight the conditions that differed significantly from the others ($p < 0.05$). In the case of comparing only two groups of values, a *t*-student test was applied and a significative difference was highlighted when $p < 0.05$.

3. Results and discussion

3.1. Graphene based nanomaterials characteristics

As the effects and fate of GBMs can be greatly influenced by their properties, the characterisation of the different materials used is essential. The characteristics of the GO and rGO used during this study are summarized in Table 1, their XRD spectrum presented in Fig. 1 and their SEM observation shown in Fig. 2. The main information from XRD data is the shift of the main peak at 11° in GO to a wide peak in rGO with a

Table 1
Characteristics of GO and rGO used during the study and compared with other GO and rGO used in studies investigating effects on microalgae. At%: atomic %; HRTEM: high resolution transmission electron microscope; TEM: transmission electron microscope; BET: Brunauer-Emett-Teller.

	GO (this study)	GO [16]	GO [17]	GO [14]	rGO (this study)	rGO [17]
Carbon content (at%)	68.62 %	66.1 %	39.1 %	–	83.01 %	62.3 %
Oxygen content (at %)	30.37 %	32.9 %	55.2 %	–	16.81 %	30.1 %
C/O	2.26	2.01	0.71	1.95	4.94	2.07
Csp2 graphene (at%)	35.5 %	–	–	–	64.5 %	–
***C*–OH/*C*–*O*–C (at%)**	24.7 %	–	–	–	7.8 %	–
C=O (at%)	2.5 %	–	–	–	5.8 %	–
O=C–O (at%)	5.3 %	–	–	–	1.3 %	–
Sat. (at%)	1.4 %	–	–	–	4.5 %	–
Number of layers (HRTEM)	1–5	–	–	–	1–5	–
Lateral size (TEM)	0.2–8 μm	–	2 μm	–	0.2–8 μm	1 μm
Surface area (BET)	152 m^2 g^{-1}	–	242 m^2 g^{-1}	–	155.7 m^2 g^{-1}	624 m^2 g^{-1}
I_D/I_G (RAMAN)	1.09 ± 0.06	–	0.86	0.98	1.26 ± 0.03	1.04

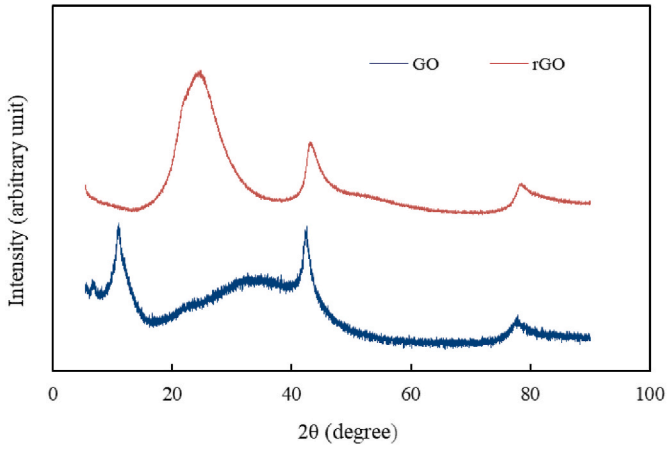

Fig. 1. XRD spectrum of GO and rGO used in this study.

maximum close to 24.8°, below 26.4° (characteristic of graphite, or fully reduced GO [28]). This evidences first that the starting material is indeed GO, but also that heating at 200 °C did not fully reduce GO. Indeed, the 200 °C thermal reduction of GO resulted in the loss of approximately half of the oxygen atoms that were in the form of *C*–OH, *C*–*O*–C and O=C–O in GO. The different oxygen contents between GO and rGO could also influence the hydrophilicity of the materials. Indeed, in a work recently published by our group using the exact same GO and rGO samples [29], Turbiscan measurements were performed to monitor the turbidity of both suspensions along all the height of the water columns and thus allowed to obtain information about the kinetics of sedimentation. The difference of stability between each sample was clearly shown. GO remained more stable in the water column than the corresponding rGO. However, these results are obtained in sea water samples. In another work, not published yet (figure SD1), the same measurement was obtained in still water and reveals a very similar behaviour (the slight difference due to the different salinity composition). Even if these measurements were unfortunately not performed in the framework of the current work, we can assume that the behaviour in our exposure medium should be similar, clearly demonstrating that GO is more hydrophilic than rGO, as expected from their respective oxygen content. This difference of stability in the water column could have a major influence on the turbidity and shading of the water column and thus on the effects on diatoms. RAMAN spectrums were also analysed and indicated an increase in the I_D/I_G ratio following the reduction. The increase of the I_D/I_G has been previously associated with the reduction of GO [30–32] but also with increased defects such as holes which are the result of loss of oxygen groups [33] and defects in edges generally due to the loss of carbon bonds [34]. The reduction did not induce changes in the dimensional properties such as the number of layers, the lateral size and surface area. The surface chemistry of rGO was modified while the morphology remained the same, making the comparison with GO especially relevant. Oxygen and carbon content were comparable to GO in the studies of Yin et al. [16] and Malina et al. [14]. rGO used by Zhao et al. [17] was more comparable to our GO, and the GO used in their study was much more oxidized, but lateral size were similar. Taken as a whole, the characteristics of the GO and rGO used in this study are in line those used in studies investigating the effects of GBMs on micro algae.

3.2. *Increased division rate of Nitzschia palea by GO*

Actual division rates of *Nitzschia palea* exposed to different doses of rGO and GO are presented in Fig. 3a and b. At the concentrations tested (0.1, 1 and 10 mg L^{-1}), rGO had no significant effect on the diatom's division rate throughout the 144 h of exposure. These results are opposite to the ones obtained in previous studies conducted on *Scenedesmus obliquus*, showing a negative effect of rGO at 72 h of exposure in presence of 10–300 mg L^{-1} [12], and on *Chlorella pyrenoidosa* after 96 h with 20–200 mg L^{-1} [17]. However, concentrations of rGO used in those studies were higher than the ones used in this present work. In the case of GO, it induced a dose dependent effect on the division rate. At 0.1 mg L^{-1}, GO had no significant effect, regardless of the incubation time. At 1 mg L^{-1}, the actual division rate increased significantly at 48 h. At 10 mg L^{-1}, division increased significantly from 24 to 144 h (TukeyHSD $p < 0.05$).

These original results obtained with GO are not in line with the literature trend showing negative effects of GO on the growth rates of

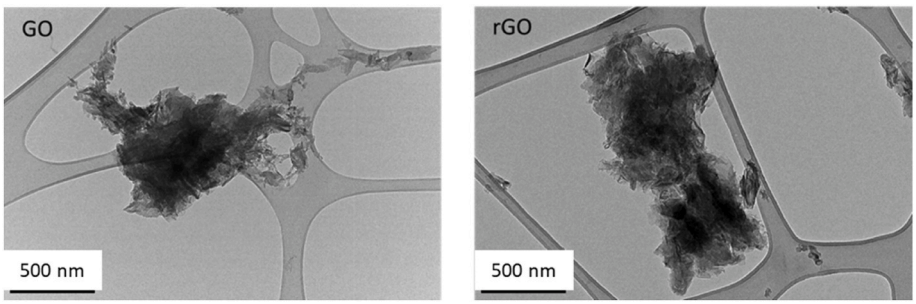

Fig. 2. TEM images of GO (left panel) and rGO (right panel).

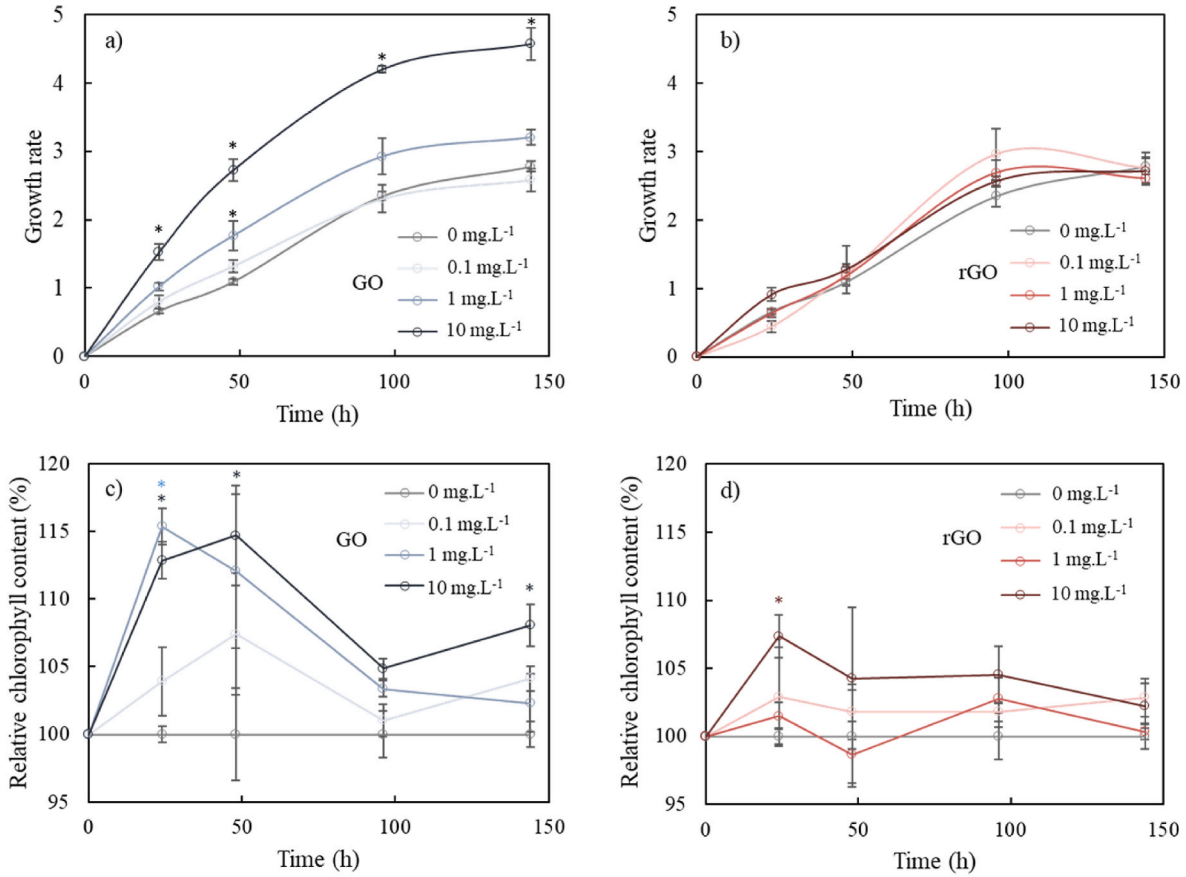

Fig. 3. Division rates of Nitzschia palea when exposed to a) GO, to b) rGO. Chlorophyll content in Nitzschia palea exposed to c) GO and d) rGO. * represents significant differences (TukeyHSD $p < 0.05$). (A colour version of this figure can be viewed online.)

micro algae such as *Raphidocelis subcapitata* with 10 and 20 mg L^{-1} [15] and with 0.39–200 mg L^{-1} [14]. Malina et al. also observed growth inhibitions with GO on the cyanobacteria *Synechococcus elongatus*. GO was also shown to have a negative effect on *Chlorella pyrenoidosa* (EC_{50}: 37.34 mg L^{-1}) [17]. GO toxicity was often attributed to the formation of reactive oxygen species (ROS) leading to membrane lipid peroxidation, but also to mechanical physical damage. Interestingly, all these results were observed on pelagic algae whereas *N. palea* is a benthic diatom. The difference of GO effect on cyanobacteria (*Microcystis aeruginosa*), green algae (*Chlorella vulgaris, Scenedesmus obliquus* and *Chlamydomonas reinhardtii*) and diatoms (*Cyclotella* sp.) was tested. Even though it was shown that the diatom was one of the less affected species, growth inhibition was observed for all species tested with GO at 10 mg L^{-1} [16]. The diatom *Cyclotella* sp. Was however not cultivated in the benthic biofilm form of life, while the biofilm form of life seems to be an important factor in the response and resistance to pollutants [35]. The only available data about the effects of GBMs on a benthic diatom was on *Nitzschia palea* exposed to FLG, showing no effect on division rate up to 10 mg L^{-1} [13]. FLG being slightly more comparable to rGO than GO in terms of oxygen content, our results obtained upon rGO exposure corroborate the study of Garacci et al., Our study suggests that the beneficial effect of GO on *Nitzschia palea* is strongly associated with its oxygen content. Although the ecotoxicity of GO and rGO had not been previously investigated on any benthic diatom species, one study investigated the effect of GO at 10 mg L^{-1} on a complex biofilm composed of a bacterial community and *Nitzschia palea* [18]. The authors reported an increase in the division rate and suggested that these benefits were due to the association with the bacterial compartment. Our study proposes another hypothesis since *Nitzschia palea* benefited alone from the presence of GO.

3.3. Chlorophyll content increase and minor shading effect upon GO exposure

The dynamics of the chlorophyll relative content along the exposure time exhibited a similar pattern to the division rates. On one hand, GO at 10 mg L^{-1} had a positive effect (Fig. 3c, TukeyHSD $p < 0.05$) on the chlorophyll content as soon as at 24 h. We also observed an increase with 1 mg L^{-1} and a non-significant increase with 0.1 mg L^{-1}. At 10 mg L^{-1}, the chlorophyll content increase was observed at each sampling point except at 96 h. On the other hand, rGO induced a chlorophyll content increase only at 10 mg L^{-1} after 24 h of exposure (Fig. 3d). These results, once again, contradict the majority of the literature. Two previous studies showed decreases of chlorophyll contents in the presence of GBMs, which were related to decreased growth rates [12,16]. *Nitzschia palea* being mainly a phototrophic organism, and while observing an increase in its division rate, the increase in the chlorophyll content could be explained by a higher photosynthetic activity to sustain growth. A similar increase in chlorophyll content was reported with 10 mg L^{-1} [18] where GO had a positive impact on the division rate of *Nitzschia palea* cultured with a bacterial consortium. Besides, in a recent study with multiwall carbon nanotubes (MWCNTs), chlorophyll contents of the green microalgae *Dunaliella salina* was found to increase while the growth was inhibited [36]. Authors suggested that this increase was a strategy for compensating the shading effect induced by nanoparticles. Shading effect was indeed reported by GO on algae [17] and also with FLG at 50 mg L^{-1} on the diatom *Nitzschia palea* [13]. The increase in chlorophyll content observed in our experiment with GO and slightly with rGO could be a compensatory response to a potential shading effect.

The results of the shading effect experiment are presented in Fig. 4a.

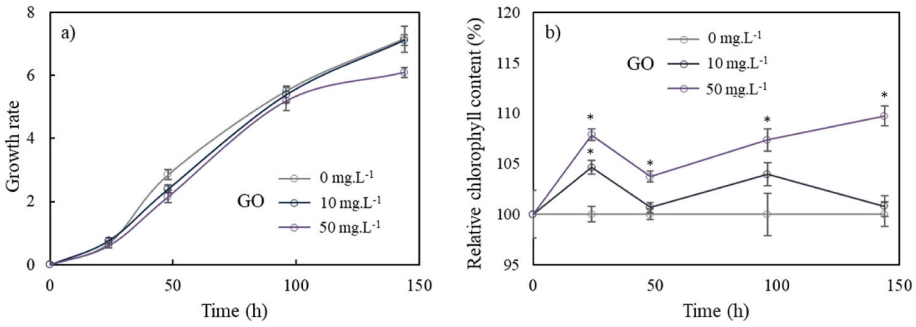

Fig. 4. *Division rate (a) and relative chlorophyll content (b) of* Nitzschia palea *when exposed to 10 and* 50 mg L^{-1} *of GO in shading conditions. * represent significant differences with the control (TukeyHSD $p < 0.05$).* (A colour version of this figure can be viewed online.)

The shading resulting from 10 to 50 mg L^{-1} of GO had no significant impact on the division rate of *Nitzschia palea* (TukeyHSD $p > 0.05$). Interestingly, the chlorophyll contents (Fig. 4b) increased with both concentrations (ranging from 4 to 10 % increase with 50 mg L^{-1}, from 1 to 6 % with 10 mg L^{-1}), with the higher concentration inducing a higher increase in the chlorophyll content. These results confirm the hypothesis that the increased chlorophyll content during a normal exposure could be a strategy for overcoming the shading effect of GO, as already suggested in the literature [36]. The different magnitude of shading effect may also explain the difference between GO and rGO effect on chlorophyll levels. As rGO is less stable in water and less dispersed (Turbiscan measurements, Supplementary Fig. 1), it has a weaker effect than GO in darkening the water column. A slight shading effect caused by rGO cannot be excluded, potentially countered by a slight increase in chlorophyll (Fig. 3d), ultimately having no impact on growth. Nevertheless, this shading compensation in presence of GO partially explained the chlorophyll content increase: after 24 h of exposure with 10 mg L^{-1} of GO, it represented +4.3 % in shading condition against +13.0 % in regular exposure. These results thus showed that the growth and chlorophyll content increase of *Nitzschia palea* did not only rely on a shading compensation but also on a contact with this GBM, either through a direct GO-diatom contact or indirectly through the biofilm matrix or the medium.

3.4. Unchanged photosynthesis efficiency

Dynamic changes in chlorophyll fluorescence yield is a non-destructive method providing information on how the absorbed energy is managed in the photosynthetic membranes, serving as a proxy for estimating the organism fitness [37]. The photosynthetic machinery is composed by two photosystems working in series. The electrons are generated at the photosystem II (PSII) and transported to photosystem I (PSI) along an electron transport chain including the primary and secondary PSII electron acceptors, namely Q_A and Q_B. A typical OJIP Chl fluorescence induction kinetics recorded with nontreated samples is displayed in Fig. 5a. The capacity of the different samples to capture photons (ABS/RC parameter) was not affected by the presence of GO (Fig. 5b) while the relative chlorophyll cellular quota increased (Fig. 3c). This suggests that the additional chlorophyll molecules were used to form additional photosynthetic units, with a light harvesting capacity (RC/ABS parameter [38] = 0.99) similar to that present in the diatoms cultured in the absence of GO (RC/ABS = 0.91, t-student $p > 0.05$). Interestingly, energy trapped by RCII (TR_0/RC parameter), the energy used for injecting electrons in the photosynthetic electron transport chain (ET_0/RC parameter) and the flux of energy dissipated as heat and/or fluorescence were not significantly different in the presence of GO when compared to the control conditions indicating that the photosynthetic capacity of the diatoms was not affected by GO.

The 77 K fluorescence spectrum of the nontreated sample presents two bands at 690 and around 712 nm (Fig. 4A), reflecting the presence of PSII and PSI, respectively [39]. The F712/F690 band ratio in control condition is 1.01. In chlorophyll *c* containing algae, this ratio varies considerably between taxa [39] and is impacted by the developmental stages [40] and the environmental conditions (Brown, 1967). The 2nd derivative spectrum reveals the spectral heterogeneity of the 712 nm band with components at 705 and 721 nm (Fig. 6b). The component at 705 nm is widely distributed among photosynthetic organisms (Supplementary Table 1). The band associated to PSII is also spectrally heterogenous with components at 650 and 667 nm, reflecting the presence of pigment-protein complexes of unknown origin. The short-wavelength fluorescence emission at 622 and 638 nm might reflect chlorophyll *c* not integrated in photosystems [40].

Qualitatively, the presence of GO does not affect the 77 K fluorescence spectrum (Fig. 6a). In the absence of reference 77 K fluorescence spectrum in the literature, it is difficult to decide how much the spectrum of *Nitzschia palea* presented in Fig. 6a is impacted directly by the presence of GO or indirectly through a delay in the assembly of the photosynthetic apparatus in the diatoms cultivated in the presence of

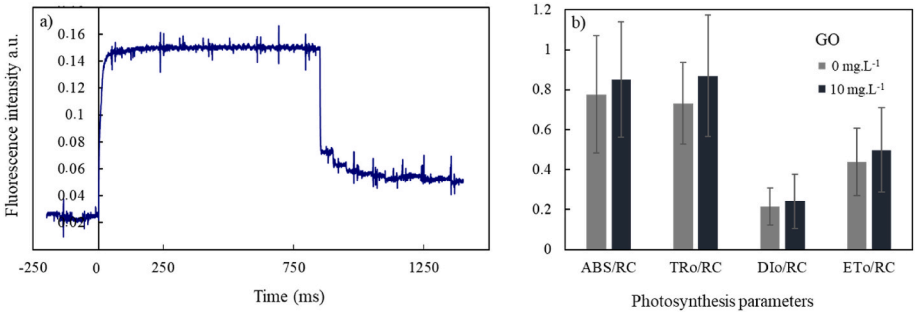

Fig. 5. a) OJIP chlorophyll fluorescence induction kinetics of Nitzschia palea; b) Means of the different fluxes per reaction centre of Nitzschia palea during the 144 h of exposure to 10 mg L^{-1} of GO compared to the control condition. RC: reaction centre; ABS: Absorbance; TRo: Trapping; DIo: Dissipation; ETo: Electron transport. (A colour version of this figure can be viewed online.)

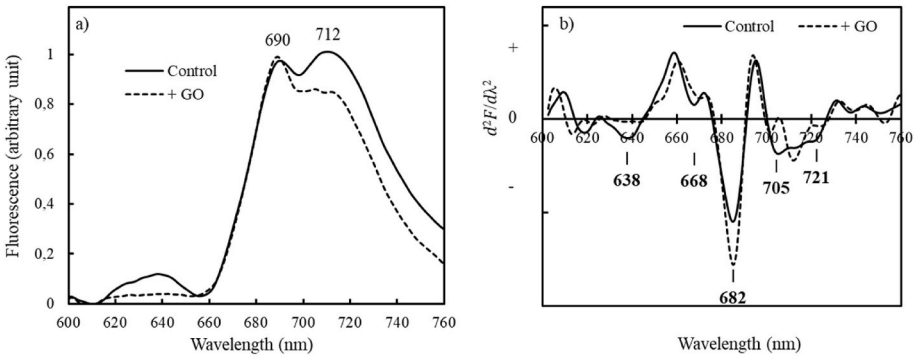

Fig. 6. a) 77 k fluorescence emission spectra of the diatom Nitzschia palea in control and exposed (10 mg L^{-1} GO) conditions. b) Second derivative spectra of the 77 k fluorescence emission spectra of Nitzschia palea in control and exposed (10 mg L^{-1} GO) conditions. (A colour version of this figure can be viewed online.)

GO. From the quantitative point of view, the F712/F690 band ratio was lower (0.84) in the presence of GO. The decrease of ratio could be interpreted by an increase of the PSII production by *Nitzschia palea* in order to optimize photon capture in an environment characterized by a shading effect. It is also possible that the decrease in the band ratio is related to a decrease in the PSII to PSI energy transfer [41], and would explain the small differences in intensity of the negative bands present in the 2nd derivative spectrum (Fig. 6b).

3.5. Sedimentation, "sticking" of GO and interactions with Nitzschia palea

To better understand the GBM-diatom interactions positively affecting the growth of *Nitzschia palea*, the GO sedimentation in the cell culture was monitored. The monitoring of OD values in the water column (Fig. 7) results revealed that the presence of diatoms influenced the sedimentation of GO. In absence of diatoms, the 40 rpm agitation of the wells was enough to stabilise and maintain the GO dispersed in the water column until 144 h. In the presence of diatoms, the OD in the wells containing 10 mg L^{-1} decreased as soon as 24 h (TukeyHSD $p < 0.05$) and reached the values of non-exposed wells at 96 h, showing a complete sedimentation of GO. Similar results were reported with FLG, but the sedimentation was faster (complete sedimentation at 24 h) [13]. This slight difference is probably due to the different physico-chemical characteristics of the GBMs: as FLG is not oxidized, it is less stable in water than GO and therefore sediments faster.

Simultaneously with GO sedimentation, its sticking in biofilm was monitored and expressed as the percentage of surface covered (Fig. 7). For concentrations below 10 mg L^{-1}, the method was not sensitive enough to detect sticking and were not represented. In presence of 10

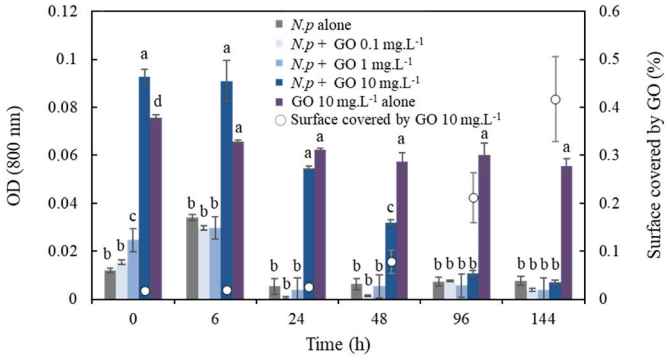

Fig. 7. Sticking of GO by Nitzschia palea through time. Bar charts represents the OD at 800 nm of the water column as a function of time. The dots represent the percentage of surface covered by GO at the bottom of the well during the exposure at 10 mg L^{-1}. Letters correspond to significantly different groups at each sampling time (TukeyHSD $p < 0.05$).

mg L^{-1}, a significant increase in the surface covered by GO was observed after 6 h of incubation (TukeyHSD $p < 0.05$), and continued to increase with time with a maximum coverage observed at 144 h. This accumulation of GO in the biofilm is in line with the sedimentation results but also with the literature showing the capability of biofilms to retain and accumulate pollutants [42,43]. These results are consistent with the chlorophyll content dynamics (Fig. 3c): the increase in chlorophyll content in the first 24 h could be partially related to the previously discussed shading effect, but after 96 h, the sedimentation and sticking of GO induced by the diatom supressed this shading effect, and the chlorophyll content decreased to reached similar values to that of control conditions.

The SEM images derived from diatom growing in control conditions clearly highlights the diatoms and their EPS network attached to the glass slide (Fig. 8A) but also holding the cells together (Fig. 8B–C). In the exposed biofilm, GO was mainly found to be directly trapped into the EPS. A fraction of GO nanoparticles was captured in the EPS covering the glass slide (Fig. 8E, green frame), giving it a granular texture. A high proportion of GO was stuck and accumulated in the EPS binding the diatoms (Fig. 8E, yellow frame and Fig. 8F). These images are in accordance and confirm the previous results showing the "sticking" of the GO in the *Nitzschia palea* biofilm. GBMs are sharp and are known to damage the membranes of microorganisms [44]. Physical damage to *Nitzschia palea* by FLG was previously observed by SEM [13]. However, GO particles are smaller than FLG and strongly stuck into the EPS produced by the diatoms. Despite all our observations (over 1000 cells), damage to diatoms frustule was never observed. This bonding of GO by EPS could greatly limit direct contact between GO and the cells, thus preventing physical damage by GO which is the main cause of membrane lipid peroxidation, oxidative stress and death. In addition to playing the role of barrier, the adhesion of GO in the EPS prevented the nanoparticles to obstruct the light received by the diatoms as it would when present in the water column. Finally, the observed accumulation of GO and its proximity with the biofilm could favour non-contact interactions between the nanoparticles and the diatom, which might explain the higher division rate observed.

3.6. Effect of GO on the bioavailability of nutrients

One of the first possible interactions between GO and the biofilm could be the fixation of vital elements at the surface of GO, increasing their bioavailability once GO were stuck in the biofilm. GBMs were already reported to interact and adsorb mineral elements during the exposure of a bacterial community [45]. In the present study, the concentrations of elements that changed significantly (TukeyHSD $p < 0.05$) with the presence of 10 mg L^{-1} GO after 24 h were the following: Al (−50.7 %), B (−7.9 %), Bi (−11.2 %), Ca (−4.9 %), Cl (−1.2 %), Fe (−3.7 %), Mg (−2.1 %), Mn (+21.1 %), Na (+0.9 %), Si (−1.1 %) and V (−9 %) (all data presented in Supplementary Table 2). A majority of

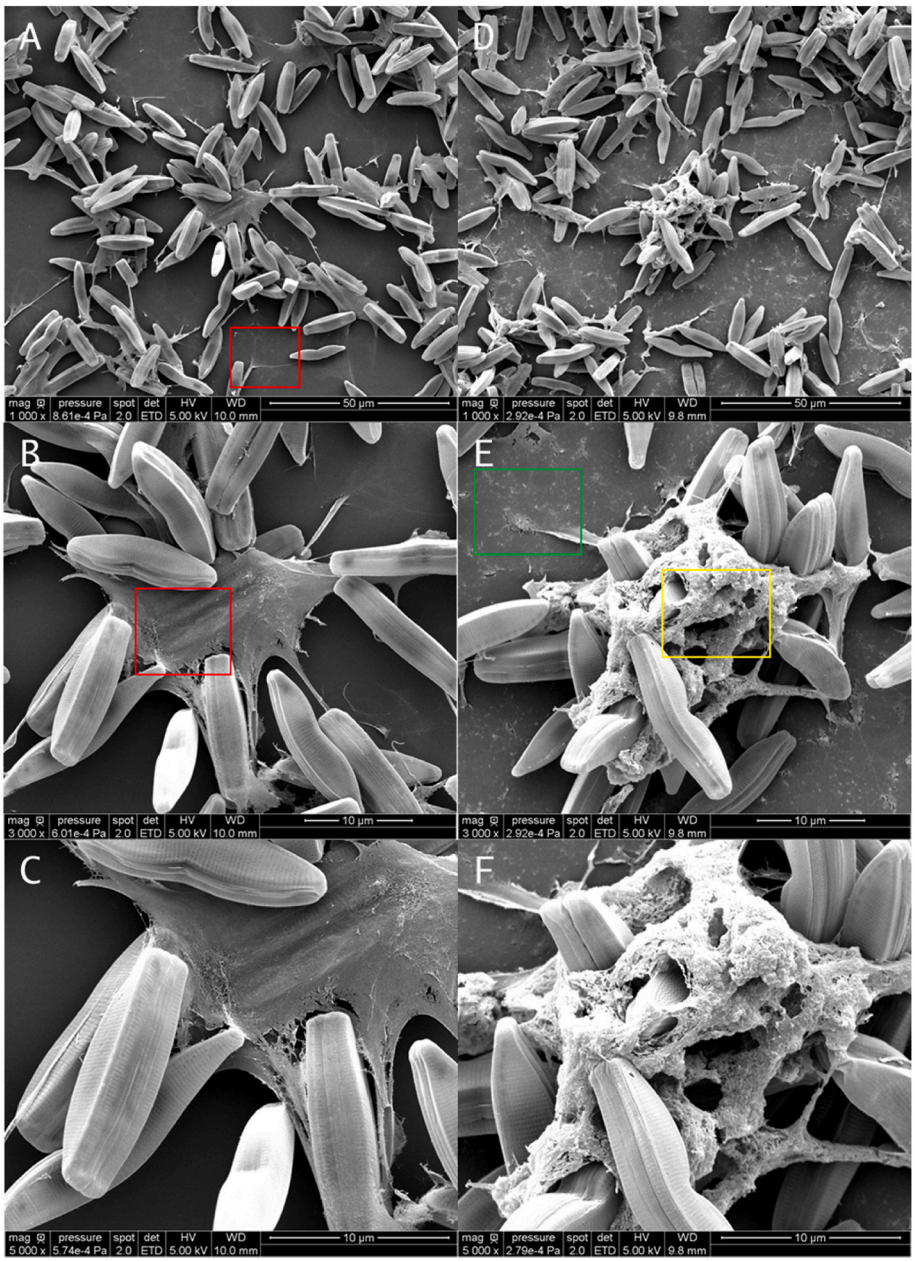

Fig. 8. SEM images of Nitzschia palea biofilm after 144 h. A, B and C are images of the control biofilm at different magnification (×1000, ×3000 and ×5000 respectively). D, E and F are images of the biofilm exposed to 10 mg L^{-1} of GO (*x*1000, ×3000 and ×5000 respectively). (A colour version of this figure can be viewed online.)

these elements varied significantly, but the absolute variation was very low (ranging from −0.0001 to −0.005 mg L^{-1}) as the majority of these elements were only present as trace in the medium. The two elements that varied in a higher extent in terms of absolute difference were Ca (−0.2 mg L^{-1}) and Cl (−0.3 mg L^{-1}). Cl and Ca have a very important role in photosynthesis [46,47]. The diatoms could have benefited from the fixation of these elements by sticking the GO in the biofilm which could induce the production of more reaction centers. But this is also very questionable as the concentration of Ca and Cl were already high in the medium (9.7 mg.$L^{-1}$and 29.6 mg L^{-1} respectively).

Interestingly, GO was shown to release Mn in the culture medium (+21.1 %). This was predictable and in accordance with the Hummers' method used in order to prepare GO, which uses potassium permanganate [19]. Even though the variation of concentration was small (approx. 0.01 mg L^{-1}), Mn is needed in small amounts and plays a crucial role in the photosystem II for water oxidation [48]. For this reason, an experiment was conducted with the culture medium supplemented with 0.01 mg L^{-1} of Mn. This had no influence on the growth rate of the diatom cells (Supplementary Fig. 2).

Even though GO had the capacity to adsorb or release different nutrients, our results thus suggest that such interactions are unlikely to explain alone the increased growth.

3.7. GO modification after diatom exposure

RAMAN spectroscopy was used in order to reveal possible changes and modifications in the GO as indicated by the I_D/I_G ratio (Fig. 9). Increase in the I_D/I_G can be associated to a reduction and loss of oxygen content in GO [31,49] but also to increased defects [50]. After 144 h of exposure, interactions between GO and the culture medium as well as cell residuals resulted in a significant increase (TukeyHSD $p < 0.05$) in the I_D/I_G ratio. The observed modification of the GO by diatom lysate

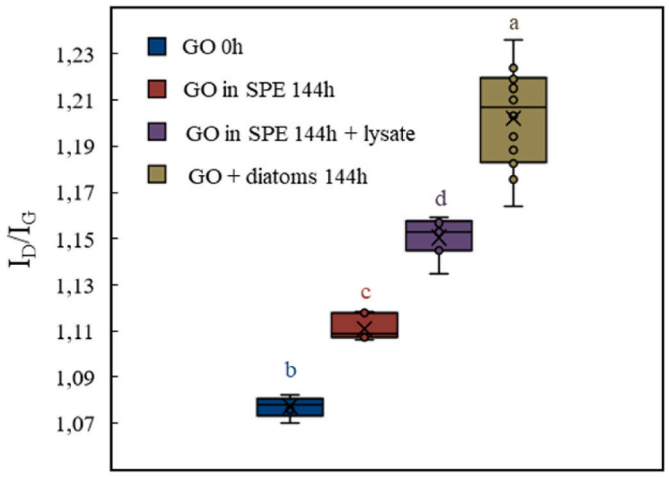

Fig. 9. I_D/I_G ratio of GO in different conditions. GO 0 h: GO diluted in SPE before exposition. GO in SPE 144 h: GO in SPE medium after 144 h. GO in SPE 144 h + lysate: GO in SPE medium after 144 h with lysed diatoms added just before analysis. GO + diatoms 144 h: GO after 144 h of exposure with Nitzschia palea. Letters correspond to significantly different groups (TukeyHSD $p < 0.05$). (A colour version of this figure can be viewed online.)

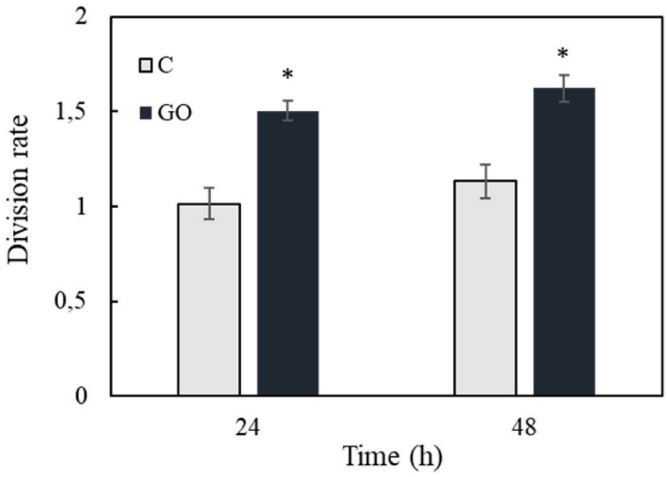

Fig. 10. Division rates in dark conditions of control and exposed Nitzschia palea. * represent significant differences between each condition at each sampling point (t-student $p < 0.05$). (A colour version of this figure can be viewed online.)

could also be the result of fast reactions between cell elements, such as enzymes, and the nanomaterial. More importantly, the increase in the ratio (TukeyHSD $p < 0.05$) when GO was exposed with diatoms (1.11–1.22) overwhelmed the cumulative effect of GO-medium and GO-cell lysate interactions, revealing that biologically active cells caused a part of this increase. A ratio increase of similar magnitude (1.40–1.55) associated to GO reduction by bacteria was previously reported in the literature [51].

While there is a growing body of literature showing the potential of bacteria to reduce GO, data on algae remain scarce or even absent. It has been shown that reduction by bacteria could result from peroxidase type enzymatic activity [52]. This type of enzymes are found in *Nitzschia palea* [53]. In our study, this enzymatic activity might have been upregulated upon exposure to GO, which could explain the reduction of GO by *Nitzschia palea*. The fact that rGO had no effect on the growth of the diatoms indicates that the oxygen-containing functional groups, more abundant in GO (Table 1), are related with the observed growth increase. The production by *N. palea* of enzymes able to reduce GO being one hypothesis, another one is that the reduction of GO would be the consequence of interactions between the EPS and the nanoparticle along the 144 h exposure. This could lead to the oxidation of the EPS and changes in their biochemical structure. As diatoms are able to assimilate energy and carbon from an external carbon source such as EPS [54], this second hypothesis could contribute to explain why the heterotrophic activity of *Nitzschia palea* was enhanced in presence of GO.

3.8. Possible enhancement of the heterotrophy of Nitzschia palea

In order to unravel the putative enhancement of heterotrophy in *Nitzschia palea*, the diatoms were exposed to GO in a dark condition in order to avoid photosynthesis and focus on the heterotrophy (Fig. 10). Exposure was carried out during 48 h, since the growth enhancement was observed during the first 48 h under dark/light conditions (subsection 2.2). The addition of GO induced a significant increase in growth after 24 h and until the end of the 48 h of exposure in the dark (t-student $p < 0.05$). This comforts our hypothesis on the possible enhancement of heterotrophic activity in *Nitzschia palea* with GO. Diatoms such as *Nitzschia palea* are well known to have a mixotrophic capacity [55]. As rGO did not have any influence on the diatom's growth, the hypothetical use of the sp2 carbon present in graphene was excluded. If it was the case, the diatom would also have benefited from the carbon in rGO, and rGO would have induced a similar increase in growth to that induced by GO. However, carbon present in the different hydroxyl, epoxy and carboxyl groups, lost during the reduction steps of GO in rGO, could represent a potential carbon source. Moreover, the EPS produced during the first 48 h before exposure settlement with a normal light/dark cycle also probably supported heterotrophy.

3.9. Neutral lipid content

During heterotrophic activities, the production and storage of lipids such as triacylglycerols (TAGs) are generally increased in diatoms [54]. This metabolic feature has led to the enhancement of the heterotrophy in diatoms, such as *Nitzschia palea,* for industrial applications [56]. In order to evaluate the neutral lipid contents in the diatoms during a classical exposure to GO, we used a Bodipy marker and flow cytometry. This marker stains neutral lipids such as TAGs in the diatom. After 24 h h of exposure, 0.1 and 1 mg L^{-1} of GO induced a significant increase in lipid content (TukeyHSD $p < 0.05$) while 10 mg L^{-1} had no effect on the lipid content (Fig. 11). The observed increase with 0.1 and 1 mg.L^{-1}could be

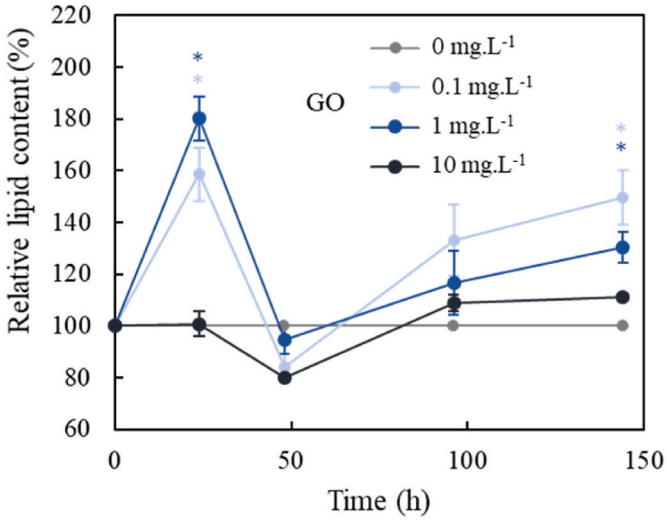

Fig. 11. Evolution of the relative lipid contents in Nitzschia palea during the 144 h exposition to GO at 0.1–1 and 10 mg L^{-1}. * represents significant differences (TukeyHSD $p < 0.05$). (A colour version of this figure can be viewed online.)

first of all the result of an increased heterotrophic activity leading to a lipid storage. After 48 h of exposure at 0.1 and 1 mg L^{-1} of GO, the lipid contents drastically dropped back to control values. It can be hypothesized that lipids hydrolysis provided the energy required for growth and EPS production. In the case of the exposure at 10 mg L^{-1}, no significant changes were observed in the lipid content. Unlike the diatoms exposed to 0.1 and 1 mg L^{-1}, those exposed to 10 mg L^{-1} grew faster. In this case, it seems that the energy obtained by increased heterotrophic activity was not used for storage but to promote cell division. A slight, but not significant decrease is observed at 48 h of exposure whatever the GO concentration. This could be, in the same case of 0.1 and 1 mg.L^{-1}, the result of the use of lipid to produce EPS, which occurs at this time in addition to cell division. Our results thus suggest a dose-dependent response of *N. Palea* response to GO: the lower concentrations (0.1 and 1 mg L^{-1}) induced a storage of the produced lipids, while with a higher concentration (10 mg L^{-1}), the increase in energy production was invested to support growth.

4. Conclusion and perspectives

To conclude, this work demonstrated that GO stimulated the division rate of the diatom *Nitzschia palea*. Higher oxygen content present in GO was a key characteristic to the observed increase, since rGO did not influence the diatom growth. The phototrophic capacity of the diatom *Nitzschia palea* increased, notably the chlorophyll contents, upon exposure to GO, with only a minor contribution of shading effect. These observations contrasted with the available literature on pelagic algae, which underlines the relevance and originality of this study conducted with a benthic diatom. Moreover, the benthic form of life of *Nitzschia palea* resulted in GO sticking into the biofilm and water column purification. Sticking induced high proximity with the nanomaterials, which led to a modification of the GO after exposure. This proximity might also explain why *Nitzschia palea* benefited from GO, probably through extracellular reactions which enhanced heterotrophic pathways. To our knowledge, no diatom before *Nitzschia palea* has been demonstrated (i) to enhance its growth upon exposure to GO and (ii) to modify GO nanoparticles throughout the exposure. The overall results and putative impacts at an ecosystem scale, such as the modulation of GO ecotoxicity and carbon cycling modification, are represented in the graphical abstract. Future works should investigate the different ongoing interactions. A transcriptomic analysis could be interesting to understand the different mechanisms occurring by focusing on expressed genes related to potential enzymes known to reduce and degrade GO, but also expressed genes related to heterotrophic pathways and EPS production/consumption. As diatoms are at the basis of trophic chains, increases in heterotrophic pathways and growth could lead to environmental imbalance and disturbance of the carbon cycle.

CRediT authorship contribution statement

Paul Braylé: Writing – review & editing, Writing – original draft, Visualization, Investigation, Formal analysis, Data curation, Conceptualization. **Eric Pinelli:** Writing – review & editing, Visualization, Validation, Supervision, Conceptualization. **Benoît Schoefs:** Writing – review & editing, Validation, Methodology, Conceptualization. **Emmanuel Flahaut:** Writing – review & editing, Resources, Investigation. **Jérôme Silvestre:** Writing – review & editing, Methodology, Conceptualization. **Laury Gauthier:** Writing – review & editing, Project administration, Funding acquisition. **Maialen Barret:** Writing – review & editing, Visualization, Validation, Supervision, Conceptualization.

Declaration of competing interest

The authors declare the following financial interests/personal relationships which may be considered as potential competing interests:

Laury Gauthier reports financial support was provided by Graphene Flagship.

Acknowledgments

Authors would like to thank Brigitte Dubreuil from the “Laboratoire de Chimie Agro-Industrielle” (LCA) for her help on the RAMAN analysis, Isabelle Fourquaux from the “Centre de Microscopie Electronique Appliquée à la Biologie” (CMEAB) for her help for the preparation of samples for the SEM imaging, the European Union’s Horizon 2020 research and innovation program under grant agreement n°881603 and finally the French Ministry of Higher Education and Research for the PhD grant n°2020–11.

Appendix A. Supplementary data

Supplementary data to this article can be found online at https://doi.org/10.1016/j.carbon.2024.119224.

References

[1] K.S. Novoselov, A.K. Geim, S.V. Morozov, D. Jiang, Y. Zhang, S.V. Dubonos, I. V. Grigorieva, A.A. Firsov, Electric field effect in atomically thin carbon films, Science, New Series 306 (2004) 666–669.
[2] X. Huang, Z. Yin, S. Wu, X. Qi, Q. He, Q. Zhang, Q. Yan, F. Boey, H. Zhang, Graphene-based materials: synthesis, characterization, properties, and applications, Small 7 (2011) 1876–1902, https://doi.org/10.1002/smll.201002009.
[3] S. Kumar, K. Chatterjee, Comprehensive review on the use of graphene-based substrates for regenerative medicine and biomedical devices, ACS Appl. Mater. Interfaces 8 (2016) 26431–26457, https://doi.org/10.1021/acsami.6b09801.
[4] T. Ch-Th, R. Manisekaran, J. Santoyo-Salazar, B. Schoefs, S. Velumani, H. Castaneda, A. Jantrania, Graphene oxide decorated TiO2 and BiVO4 nanocatalysts for enhanced visible-light-driven photocatalytic bacterial inactivation, J. Photochem. Photobiol. Chem. 418 (2021) 113374, https://doi.org/10.1016/j.jphotochem.2021.113374.
[5] K. Lü, G. Zhao, X. Wang, A brief review of graphene-based material synthesis and its application in environmental pollution management, Chin. Sci. Bull. 57 (2012) 1223–1234, https://doi.org/10.1007/s11434-012-4986-5.
[6] T. Schmaltz, L. Wormer, U. Schmoch, H. Döscher, Graphene roadmap briefs (No. 3): meta-market analysis 2023, 2D Mater. 11 (2024) 022002, https://doi.org/10.1088/2053-1583/ad1e78.
[7] L. De Marchi, C. Pretti, B. Gabriel, P.A.A.P. Marques, R. Freitas, V. Neto, An overview of graphene materials: properties, applications and toxicity on aquatic environments, Sci. Total Environ. 631–632 (2018) 1440–1456, https://doi.org/10.1016/j.scitotenv.2018.03.132.
[8] T.Y. Sun, N.A. Bornhöft, K. Hungerbühler, B. Nowack, Dynamic probabilistic modeling of environmental emissions of engineered nanomaterials, Environ. Sci. Technol. 50 (2016) 4701–4711, https://doi.org/10.1021/acs.est.5b05828.
[9] H.M. Hegab, A. ElMekawy, L. Zou, D. Mulcahy, C.P. Saint, M. Ginic-Markovic, The controversial antibacterial activity of graphene-based materials, Carbon 105 (2016) 362–376, https://doi.org/10.1016/j.carbon.2016.04.046.
[10] S. Szunerits, R. Boukherroub, Antibacterial activity of graphene-based materials, J. Mater. Chem. B 4 (2016) 6892–6912, https://doi.org/10.1039/C6TB01647B.
[11] A.-S. Benoiston, F.M. Ibarbalz, L. Bittner, L. Guidi, O. Jahn, S. Dutkiewicz, C. Bowler, The evolution of diatoms and their biogeochemical functions, Phil. Trans. Biol. Sci. 372 (2017) 20160397, https://doi.org/10.1098/rstb.2016.0397.
[12] S. Du, P. Zhang, R. Zhang, Q. Lu, L. Liu, X. Bao, H. Liu, Reduced graphene oxide induces cytotoxicity and inhibits photosynthetic performance of the green alga Scenedesmus obliquus, Chemosphere 164 (2016) 499–507, https://doi.org/10.1016/j.chemosphere.2016.08.138.
[13] M. Garacci, M. Barret, F. Mouchet, C. Sarrieu, P. Lonchambon, E. Flahaut, L. Gauthier, J. Silvestre, E. Pinelli, Few Layer Graphene sticking by biofilm of freshwater diatom Nitzschia palea as a mitigation to its ecotoxicity, Carbon 113 (2017) 139–150, https://doi.org/10.1016/j.carbon.2016.11.033.
[14] T. Malina, E. Maršálková, K. Holá, J. Tuček, M. Scheibe, R. Zbořil, B. Maršálek, Toxicity of graphene oxide against algae and cyanobacteria: nanoblade-morphology-induced mechanical injury and self-protection mechanism, Carbon 155 (2019) 386–396, https://doi.org/10.1016/j.carbon.2019.08.086.
[15] P.F.M. Nogueira, D. Nakabayashi, V. Zucolotto, The effects of graphene oxide on green algae Raphidocelis subcapitata, Aquat. Toxicol. 166 (2015) 29–35, https://doi.org/10.1016/j.aquatox.2015.07.001.
[16] J. Yin, W. Fan, J. Du, W. Feng, Z. Dong, Y. Liu, T. Zhou, The toxicity of graphene oxide affected by algal physiological characteristics: a comparative study in cyanobacterial, green algae, diatom, Environ. Pollut. 260 (2020) 113847, https://doi.org/10.1016/j.envpol.2019.113847.
[17] J. Zhao, X. Cao, Z. Wang, Y. Dai, B. Xing, Mechanistic understanding toward the toxicity of graphene-family materials to freshwater algae, Water Res. 111 (2017) 18–27, https://doi.org/10.1016/j.watres.2016.12.037.
[18] L. Evariste, P. Braylé, F. Mouchet, J. Silvestre, L. Gauthier, E. Flahaut, E. Pinelli, M. Barret, Graphene-based nanomaterials modulate internal biofilm interactions

and microbial diversity, Front. Microbiol. 12 (2021), https://doi.org/10.3389/fmicb.2021.623853.
[19] W.S. Hummers, R.E. Offeman, Preparation of graphitic oxide, J. Am. Chem. Soc. 80 (1958) 1339, https://doi.org/10.1021/ja01539a017, 1339.
[20] L.J. Hazeem, M. Bououdina, E. Dewailly, C. Slomianny, A. Barras, Y. Coffinier, S. Szunerits, R. Boukherroub, Toxicity effect of graphene oxide on growth and photosynthetic pigment of the marine alga Picochlorum sp. during different growth stages, Environ. Sci. Pollut. Res. 24 (2017) 4144–4152, https://doi.org/10.1007/s11356-016-8174-z.
[21] X. Hu, S. Ouyang, L. Mu, J. An, Q. Zhou, Effects of graphene oxide and oxidized carbon nanotubes on the cellular division, microstructure, uptake, oxidative stress, and metabolic profiles, Environ. Sci. Technol. 49 (2015) 10825–10833, https://doi.org/10.1021/acs.est.5b02102.
[22] Z. Yan, X. Yang, I. Lynch, F. Cui, Comparative evaluation of the mechanisms of toxicity of graphene oxide and graphene oxide quantum dots to blue-green algae Microcystis aeruginosa in the aquatic environment, J. Hazard Mater. 425 (2022) 127898, https://doi.org/10.1016/j.jhazmat.2021.127898.
[23] L. Verneuil, J. Silvestre, F. Mouchet, E. Flahaut, J.-C. Boutonnet, F. Bourdiol, T. Bortolamiol, D. Baqué, L. Gauthier, E. Pinelli, Multi-walled carbon nanotubes, natural organic matter, and the benthic diatom Nitzschia palea : “A sticky story.”, Nanotoxicology 9 (2015) 219–229, https://doi.org/10.3109/17435390.2014.918202.
[24] F. Lynch, A. Santana-Sánchez, M. Jämsä, K. Sivonen, E.-M. Aro, Y. Allahverdiyeva, Screening native isolates of cyanobacteria and a green alga for integrated wastewater treatment, biomass accumulation and neutral lipid production, Algal Res. 11 (2015) 411–420, https://doi.org/10.1016/j.algal.2015.05.015.
[25] D. Vanhauteghem, K. Audenaert, K. Demeyere, F. Hoogendoorn, G.P.J. Janssens, E. Meyer, Flow cytometry, a powerful novel tool to rapidly assess bacterial viability in metal working fluids: proof-of-principle, PLoS One 14 (2019), https://doi.org/10.1371/journal.pone.0211583.
[26] A. Stirbet, Govindjee, On the relation between the Kautsky effect (chlorophyll a fluorescence induction) and Photosystem II: basics and applications of the OJIP fluorescence transient, J. Photochem. Photobiol., B: Biology, Special Issue on Recent Progress in the Studies of Structure and Function of Photosystem II 104 (2011) 236–257, https://doi.org/10.1016/j.jphotobiol.2010.12.010.
[27] B. Schoefs, M. Bertrand, F. Franck, Spectroscopic properties of protochlorophyllide analyzed in situ in the course of etiolation and in illuminated leaves ¶, Photochem. Photobiol. 72 (2000) 85–93, https://doi.org/10.1562/0031-8655(2000)0720085SPOPAI2.0.CO2.
[28] L. Stobinski, B. Lesiak, A. Malolepszy, M. Mazurkiewicz, B. Mierzwa, J. Zemek, P. Jiricek, I. Bieloshapka, Graphene oxide and reduced graphene oxide studied by the XRD, TEM and electron spectroscopy methods, J. Electron. Spectrosc. Relat. Phenom. 195 (2014), https://doi.org/10.1016/j.elspec.2014.07.003.
[29] A. Mottier, M. Légnani, F. Candaudap, E. Flahaut, F. Mouchet, L. Gauthier, L. Evariste, Graphene oxide worsens copper-mediated embryo-larval toxicity in the pacific oyster while reduced graphene oxide mitigates the effects, Chemosphere 335 (2023) 139140, https://doi.org/10.1016/j.chemosphere.2023.139140.
[30] V. Balaji Mohan, Debes Stamm, M. Bhattacharyya, D. Liu, K. Jayaraman, Improvements in electronic structure and properties of graphene derivatives, Adv. Mater. Lett. 7 (2016) 421–429, https://doi.org/10.5185/amlett.2016.6123.
[31] C.R. Minitha, R.T. Rajendrakumar, Synthesis and characterization of reduced graphene oxide, Adv. Mater. Res. 678 (2013) 56–60. https://doi.org/10.4028/www.scientific.net/AMR.678.56.
[32] A. Wróblewska, A. Dużyńska, J. Judek, L. Stobiński, K. Żerańska, A.P. Gertych, M. Zdrojek, Statistical analysis of the reduction process of graphene oxide probed by Raman spectroscopy mapping, J. Phys. Condens. Matter 29 (2017) 475201, https://doi.org/10.1088/1361-648X/aa92fe.
[33] O. Akhavan, Bacteriorhodopsin as a superior substitute for hydrazine in chemical reduction of single-layer graphene oxide sheets, Carbon 81 (2015) 158–166, https://doi.org/10.1016/j.carbon.2014.09.044.
[34] M.D. Bhatt, H. Kim, G. Kim, Various defects in graphene: a review, RSC Adv. 12 (2022) 21520–21547, https://doi.org/10.1039/d2ra01436j.
[35] L.V. Evans, Biofilms: Recent Advances in Their Study and Control, CRC Press, 2003.
[36] H. Zamani, Effect of co-exposure of multi-wall carbon nanotubes and cadmium on microalga Dunaliella salina, J. Appl. Phycol. 35 (2023) 661–671, https://doi.org/10.1007/s10811-023-02908-1.
[37] K. Roháček, J. Soukupová, M. Bartak, Chlorophyll fluorescence: a wonderful tool to study plant physiology and plant stress, Plant Cell Compartments - Selected Topics (2008) 41–104.
[38] A.J. Clark, W. Landolt, J.B. Bucher, R.J. Strasser, Beech (Fagus sylvatica) response to ozone exposure assessed with a chlorophyll a fluorescence performance index, Environ. Pollut. 109 (2000) 501–507, https://doi.org/10.1016/S0269-7491(00)00053-1.
[39] K. Sugahara, N. Murata, A. Takamiya, Fluorescence of chlorophyll in brown algae and diatoms, Plant Cell Physiol. 12 (1971) 377–385, https://doi.org/10.1093/oxfordjournals.pcp.a074631.
[40] M. Lamote, E. Darko, B. Schoefs, Y. Lemoine, Assembly of the photosynthetic apparatus in embryos from Fucus serratus L, Photosynth. Res. 77 (2003) 45–52, https://doi.org/10.1023/A:1024999024157.
[41] W.L. Butler, M. Kitajima, Energy transfer between photosystem II and photosystem I in chloroplasts, Biochim. Biophys. Acta Bioenerg. 396 (1975) 72–85, https://doi.org/10.1016/0005-2728(75)90190-5.
[42] M. Schorer, M. Eisele, Accumulation of inorganic and organic pollutants by biofilms in the aquatic environment, Water Air Soil Pollut. 99 (1997) 651–659, https://doi.org/10.1007/BF02406904.
[43] U. Tahir, A. Yasmin, Role of bacterial extracellular polymeric substances (EPS) in uptake and accumulation of co-contaminants, Int. J. Environ. Sci. Technol. 16 (2019) 8081–8092, https://doi.org/10.1007/s13762-019-02360-0.
[44] X. Zou, L. Zhang, Z. Wang, Y. Luo, Mechanisms of the antimicrobial activities of graphene materials, J. Am. Chem. Soc. 138 (2016) 2064–2077, https://doi.org/10.1021/jacs.5b11411.
[45] J. Du, X. Hu, Q. Zhou, Graphene oxide regulates the bacterial community and exhibits property changes in soil, RSC Adv. 5 (2015) 27009–27017, https://doi.org/10.1039/C5RA01045D.
[46] N. Terry, Photosynthesis, growth, and the role of chloride 1 2, Plant Physiol. 60 (1977) 69–75, https://doi.org/10.1104/pp.60.1.69.
[47] Q. Wang, S. Yang, S. Wan, X. Li, The significance of calcium in photosynthesis, Int. J. Mol. Sci. 20 (2019) 1353, https://doi.org/10.3390/ijms20061353.
[48] M.M. Najafpour, I. Zaharieva, Z. Zand, S. Maedeh Hosseini, M. Kouzmanova, M. Hołyńska, I. Tranca, A.W. Larkum, J.-R. Shen, S.I. Allakhverdiev, Water-oxidizing complex in Photosystem II: its structure and relation to manganese-oxide based catalysts, Coord. Chem. Rev. 409 (2020) 213183, https://doi.org/10.1016/j.ccr.2020.213183.
[49] Y. Shen, S. Yang, P. Zhou, Q. Sun, P. Wang, L. Wan, J. Li, L. Chen, X. Wang, S. Ding, D.W. Zhang, Evolution of the band-gap and optical properties of graphene oxide with controllable reduction level, Carbon 62 (2013) 157–164, https://doi.org/10.1016/j.carbon.2013.06.007.
[50] R. Beams, L.G. Cançado, L. Novotny, Raman characterization of defects and dopants in graphene, J. Phys. Condens. Matter 27 (2015) 083002, https://doi.org/10.1088/0953-8984/27/8/083002.
[51] M. Boutchich, A. Jaffré, D. Alamarguy, J. Alvarez, A. Barras, Y. Tanizawa, R. Tero, H. Okada, T.V. Thu, J.P. Kleider, A. Sandhu, Characterization of graphene oxide reduced through chemical and biological processes, J. Phys.: Conf. Ser. 433 (2013) 012001, https://doi.org/10.1088/1742-6596/433/1/012001.
[52] M. Chen, X. Qin, G. Zeng, Biodegradation of carbon nanotubes, graphene, and their derivatives, Trends in Biotechnology, Special Issue: Environmental Biotechnology 35 (2017) 836–846, https://doi.org/10.1016/j.tibtech.2016.12.001.
[53] T.L.N. Nguyen-Deroche, A. Caruso, T.T. Le, T.V. Bui, B. Schoefs, G. Tremblin, A. Morant-Manceau, Zinc affects differently growth, photosynthesis, antioxidant enzyme activities and phytochelatin synthase expression of four marine diatoms, Sci. World J. (2012) e982957, https://doi.org/10.1100/2012/982957, 2012.
[54] V. Villanova, C. Spetea, Mixotrophy in diatoms: molecular mechanism and industrial potential, Physiol. Plantarum 173 (2021) 603–611, https://doi.org/10.1111/ppl.13471.
[55] N.C. Tuchman, M.A. Schollett, S.T. Rier, P. Geddes, Differential heterotrophic utilization of organic compounds by diatoms and bacteria under light and dark conditions, Hydrobiologia 561 (2006) 167–177, https://doi.org/10.1007/s10750-005-1612-4.
[56] H.E. Touliabah, M.I. Abdel-Hamid, A.W. Almutairi, Long-term monitoring of the biomass and production of lipids by Nitzschia palea for biodiesel production, Saudi J. Biol. Sci. 27 (2020) 2038–2046, https://doi.org/10.1016/j.sjbs.2020.04.014.